Stem Cell Reports
Article
OPEN ACCESS

Direct Conversion of Fibroblasts into Functional Astrocytes by Defined Transcription Factors

Massimiliano Caiazzo,[1,10,*] Serena Giannelli,[1] Pierluigi Valente,[2] Gabriele Lignani,[3] Annamaria Carissimo,[4] Alessandro Sessa,[1] Gaia Colasante,[1] Rosa Bartolomeo,[4,5] Luca Massimino,[1] Stefano Ferroni,[6] Carmine Settembre,[4,5,7,8,9] Fabio Benfenati,[2,3] and Vania Broccoli[1,*]

[1]Stem Cell and Neurogenesis Unit, Division of Neuroscience, San Raffaele Scientific Institute, Milan 20132, Italy
[2]Section of Physiology, Department of Experimental Medicine, University of Genoa and National Institute of Neuroscience, 16132 Genoa, Italy
[3]Department of Neuroscience and Brain Technologies, Italian Institute of Technology, 16132 Genoa, Italy
[4]Telethon Institute of Genetics and Medicine, Naples 80131, Italy
[5]Dulbecco Telethon Institute
[6]Department of Pharmacy and Biotechnology, University of Bologna, Bologna 40126, Italy
[7]Department of Molecular and Human Genetics, Baylor College of Medicine, Houston, TX 77030, USA
[8]Jan and Dan Duncan Neurological Research Institute, Texas Children's Hospital, Houston, TX 77030, USA
[9]Medical Genetics, Department of Medical and Translational Science Unit, Federico II University, Via Pansini 5, 80131 Naples, Italy
[10]Present address: Institute of Bioengineering, Ecole Polytechnique Fédérale de Lausanne, Lausanne 1015, Switzerland
*Correspondence: massimiliano.caiazzo@epfl.ch (M.C.), broccoli.vania@hsr.it (V.B.)
http://dx.doi.org/10.1016/j.stemcr.2014.12.002

SUMMARY

Direct cell reprogramming enables direct conversion of fibroblasts into functional neurons and oligodendrocytes using a minimal set of cell-lineage-specific transcription factors. This approach is rapid and simple, generating the cell types of interest in one step. However, it remains unknown whether this technology can be applied to convert fibroblasts into astrocytes, the third neural lineage. Astrocytes play crucial roles in neuronal homeostasis, and their dysfunctions contribute to the origin and progression of multiple human diseases. Herein, we carried out a screening using several transcription factors involved in defining the astroglial cell fate and identified NFIA, NFIB, and SOX9 to be sufficient to convert with high efficiency embryonic and postnatal mouse fibroblasts into astrocytes (iAstrocytes). We proved both by gene-expression profiling and functional tests that iAstrocytes are comparable to native brain astrocytes. This protocol can be then employed to generate functional iAstrocytes for a wide range of experimental applications.

INTRODUCTION

Direct cell-reprogramming technology is based on the dominant action of cell-lineage transcription factors (TFs) in converting adult somatic cells into different cell types (Graf and Enver, 2009). This technique represents a promising avenue in the field of regenerative medicine, with the potential to generate cellular sources suitable for cell-replacement therapies (Chambers and Studer, 2011). In fact, since the groundbreaking discovery of the induced pluripotent stem cells (iPSCs) (Takahashi and Yamanaka, 2006), increasing approaches of direct cell reprogramming have been established, culminating with the development of induced cellular types for neurons, cardiomyocytes, and hepatocytes (Vierbuchen et al., 2010; Ieda et al., 2010; Huang et al., 2011). In addition, we and others employed the forced expression of defined sets of TFs to generate specific induced neuronal sublineages for dopaminergic, cholinergic, and motor neurons (Caiazzo et al., 2011; Pfisterer et al., 2011; Kim et al., 2002; Son et al., 2011; Liu et al., 2013; Theka et al., 2013). More recently, two groups succeeded in the generation of induced oligodendrocyte precursors by direct conversion of fibroblasts (Najm et al., 2013; Yang et al., 2013). Surprisingly, to date, there is no report for the generation of astrocyte by means of direct cell reprogramming. Astrocytes are the most-abundant cell type in the CNS and a critical neural cell type responsible for the maintenance of brain homeostasis. Indeed, they play irreplaceable roles in neurotransmitter trafficking and recycling, nutrient and ion metabolism, regulation of blood supply, release of transmitters and growth factors, and protection against oxidative stress (Molofsky et al., 2012). Consistent with such a variety of fundamental functions exerted by astrocytes in supporting neuronal survival and function, astrocyte dysfunctions have been found to contribute to several neurological diseases, such as epilepsy, amyotrophic lateral sclerosis (ALS), Alzheimer's disease, lysosomal storage diseases (Di Malta et al., 2012), and Rett syndrome (Molofsky et al., 2012). Conversely, recent data showed that transplanted astrocyte progenitors display robust survival and differentiation in the host brain and are able to decelerate the disease course in ALS and Alzheimer's disease models (Lepore et al., 2008; Pihlaja et al., 2008). However, current protocols rely on the isolation of astrocyte progenitors from neonatal brains with serious limitations for any therapeutic approach as the paucity of cell supply and unmatched immunoprofile with the host, leading to immune reaction and possible rejection after

transplantation. Cell-reprogramming approaches, by generating astrocytes starting from adult skin fibroblasts from an immunomatched or autologous source, can represent a promising alternative system for overcoming those bottlenecks. Notably, procedures of direct iPSC differentiation into astrocytes have been established only very recently (Krencik et al., 2011; Emdad et al., 2012; Juopperi et al., 2012; Roybon et al., 2013; Serio et al., 2013; Shaltouki et al., 2013). However, these approaches rely on the previous generation of stable and mutation-free iPSC lines, and the cell differentiation protocols are considerably time-consuming, complex, and required extensive time up to 180 days. We therefore considered that a direct reprogramming approach could have interesting advantages, providing a more practical procedure to generate astrocyte-like cells. Indeed, after the identification of the reprogramming cocktail composed by the astroglial TFs NFIA, NFIB, and SOX9, we defined a straightforward and fast (~2 weeks) protocol to generate induced astrocytes (iAstrocytes) derived from mouse embryonic and postnatal fibroblasts. Our experiments indicate that iAstrocyte molecular phenotype and biological functions closely recapitulate that of native astrocytes, thus validating the direct reprogramming technology as an alternative for the generation of astrocytes.

RESULTS

Defining the Minimal Set of TFs Able to Convert Fibroblasts to an Astrocytic Cell Fate

To generate iAstrocytes, we initially performed a literature data mining for selecting a first pool of eight candidate TFs known to play relevant roles in astrocyte differentiation and maintenance during nervous system development (Rowitch, 2004; Deneen et al., 2006; Rowitch and Kriegstein, 2010). In addition, we added six additional candidate TFs that exhibit a selective expression in astrocytes when compared to the global gene-expression profiles of neurons and oligodendrocytes (Lovatt et al., 2007; Cahoy et al., 2008; Doyle et al., 2008; Najm et al., 2013). Thus, we selected a total of 14 TFs (SOX2, SOX9, PAX6, NKX6.1, OLIG1, OLIG2, NFIA, NFIB, NFIX, HES1, HES5, NICD, TAL1, and PRDM16). Their coding regions were individually cloned into doxycycline (dox)-inducible lentiviral vectors, and each lentivirus was used to infect mouse embryonic fibroblasts (MEFs). The day after the infection, MEF culture medium was replaced with fresh medium supplemented with dox. After 12 days of dox exposure, the activation of the well-known astrocyte markers GFAP and S100B was assessed by immunostaining in the infected cell culture. Interestingly, only NFIA, NFIB, and SOX9 among all 14 candidate TFs induced a significant amount of S100B-positive cells, as well as a relative smaller number of GFAP-positive cells. On the contrary, GFP infected or not infected (control) MEFs did not show any relevant expression of these two astrocyte-specific markers (Figure S1A available online). In order to confirm the presence of GFAP-positive cells and develop a system for isolating them, we set up a genetic cell-fate-tracing method selective for the astrocyte cell lineage by using MEFs derived from the hGFAP-Cre;ROSA26-stop-flox-yellow fluorescent protein (YFP) double-transgenic mice. Fluorescence-activated cell sorting (FACS) analysis confirmed the presence of YFP-positive cells after infection with NFIA, NFIB, or SOX9 (data not shown). We then combined the three factors NFIA, NFIB, and SOX9 (hereafter abbreviated as A, B, and S9) in different groups for identifying the most-performing combination in giving the highest efficiency of astrocyte conversion. Among all the possible factor combinations (AB, AS9, BS9, and ABS9), ABS9 cocktail generated the largest number of GFAP- and S100B-positive cells, as shown in Figures S1B–S1D. We confirmed this finding also by FACS analysis using the hGFAP-Cre;ROSA26-stop-flox-YFP double-transgenic MEFs, estimating in ~15% the total number of YFP-positive cells (Figures 1A and S1D). Importantly, no other factor added to this combination enabled any evident increase of the reprogrammed cell number (data not shown), concluding that ABS9 is the minimal and sufficient set of TFs eliciting a sustained conversion of MEFs into iAstrocytes. Closer inspection of ABS9 iAstrocytes confirms their round cell shape, resembling somatic astrocyte morphology and the coexpression of both the GFAP and S100B proteins in a vast fraction of them (Figures 1B, 1C, 1E, 1F, and 1H). Conversely, very few (<0.2%) S100B-positive cells and no GFAP-positive cells were detected in the GFP-transduced cell population (Figures 1D and 1G). As shown in Figure 1I, iAstrocytes also expressed high levels of the main astrocytic glutamate transporter GLT-1 (National Center for Biotechnology Information: SLC1A2). Quantitative studies determined that infected MEFs activated S100B in high numbers (21%) and that GFAP (16%) and GLT-1 (11%) were found in large subgroups of cells always colocalizing with S100B (Figure 1J; data not shown).

In order to characterize the dynamics involved in iAstro reprogramming, we analyzed the conversion at different time points by immunostaining and quantitative RT-PCR (qRT-PCR). The results of this experiment showed that neither OCT4 nor SOX2 proteins are ever expressed (data not shown) and also the transcriptional analysis did not detect any other embryonic stem cell (ESC) or neural stem cell (NSC) marker, with the only exception of *Tlx* and *Pax6* that are minimally increased only at day 1 of the reprogramming protocol (Figures S2A–S2I). These results indicate that iAstro-reprogramming process is

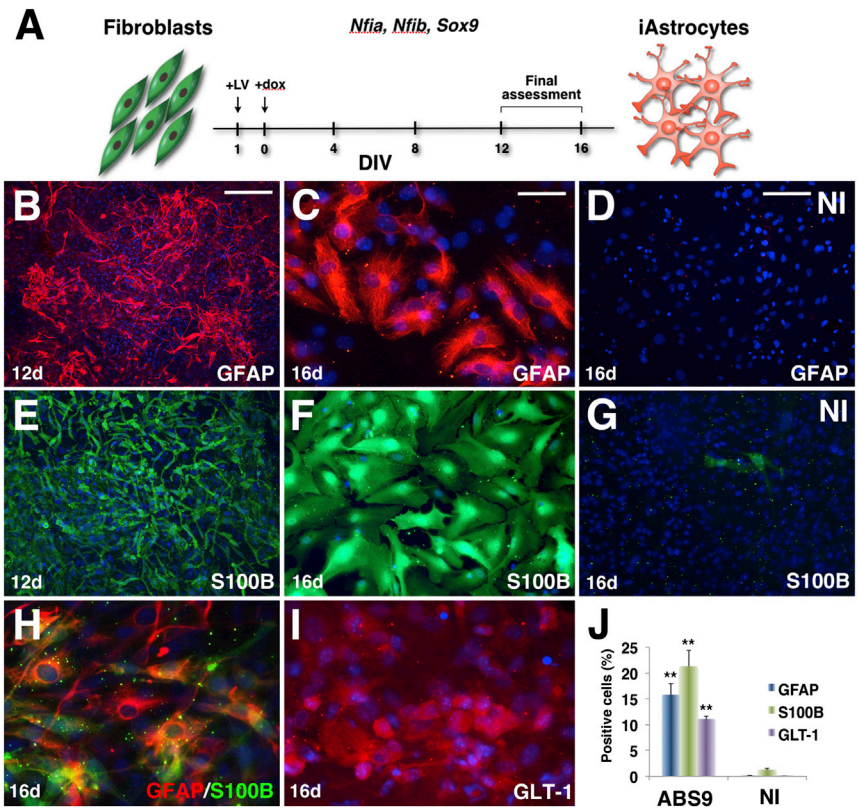

Figure 1. NFIA, NFIB, and SOX9 Efficiently Reprogram Mouse Fibroblasts into iAstrocytes

(A) Schematic representation of the one-step differentiation protocol. DIV, days in vitro.

(B–D) Analysis of GFAP immunoreactivity in reprogrammed and control (noninfected [NI]) fibroblasts (d, days after infection).

(E–G) Analysis of S100B immunoreactivity in reprogrammed and control fibroblasts.

(H) Coimmunostaining of GFAP and S100B in iAstrocytes.

(I) Immunocytochemical analysis for GLT-1 in iAstrocytes.

(J) Quantification of GFAP, S100B, and GLT-1-positive cells in iAstrocytes (ABS9) and control fibroblasts. Cells nuclei are stained with DAPI.

Data are expressed as means ± SEM. **$p < 0.01$. The scale bar represents 20 μm (C, F, H, and I) and 100 μm (B, D, E, and G). Five independent experiments are represented in (J). See also Figures S1–S4.

indeed direct, with no intermediate states resembling ESCs or NSCs. In line with this hypothesis, both *Gfap* and *S100b* expression are gradually increased since the first day after transgene activation (Figures S2J and S2K). Despite that GFAP expression was undetectable in MEFs, the STAT3-binding site on the *Gfap* promoter was often found demethylated in bisulfite-sequencing analysis, indicating that its repression is mediated by different mechanisms rather than DNA methylation in these cells (Figure S2L).

Subsequently, we analyzed the iAstro-proliferative capability, and indeed, a large fraction of iAstrocytes exhibited some proliferative capacity as confirmed by the expression of the cell-cycle marker Ki67 (Figures S3A–S3D) in expanding clusters of reprogrammed cells. In fact, reprogrammed cells could be passaged for at least eight times in the dish, whereas most of them kept showing GFAP and S100B immunoreactivity (Figures S3E and S3F).

To confirm their gliogenic-inducing activity, *Nfia*, *Nfib*, and *Sox9* were expressed in the developing cerebral cortex by means of in utero electroporation. With this method, cortical progenitors were targeted for exogenous gene expression at an embryonic stage when they are exclusively generating neurons. Mouse embryos were electroporated at embryonic day 13.5 (E13.5), and targeted cortices were analyzed at E18.5. Progenitors targeted for expression of *Nfia*, *Nfib*, or *Sox9* gene alone behaved similarly to enhanced-GFP-electroporated control cells, being capable of migrating radially in the cortical mantle and initiating neuronal differentiation; in fact, the fraction of the GFP+ cells that remained out of the cortical plate (CP) was similarly low in the four conditions (GFP 15.5% ± 2.3%; *Nfia* 13.2% ± 1.1%; *Nfib* 16.1% ± 2.9%; *Sox9* 13.2% ± 4.1%; Figures S4A–S4C, S4E–S4G, S4I–S4K, S4M–S4O, and S4Q–S4S; data not shown). In contrast, expression of the ABS9 gene combination arrested or delayed the migration of a significant number of targeted progenitors (non-CP GFP+ cells 75.2% ± 6.4%; $p < 0.001$; arrows in Figure S4H) and some of them strongly activated the expression of S100B (arrows in Figures S4L, S4P, and S4T). The low percentage of targeted cells expressing S100B (9.6% ± 3.4%) could be explained by the reduced probability of targeting each cell with the four independent plasmids (ABS9 and GFP). However, it preserves high importance because the forced expression of each single gene alone was insufficient to ectopically activate S100B, indicating that the three factors act synergistically to promote S100B expression in vivo. These results demonstrate that the three factors NFIA, NFIB, and SOX9 are capable and sufficient to activate a mature astrocytic gene program both in skin fibroblasts in vitro as well as in neuron fated-neuronal progenitors in vivo.

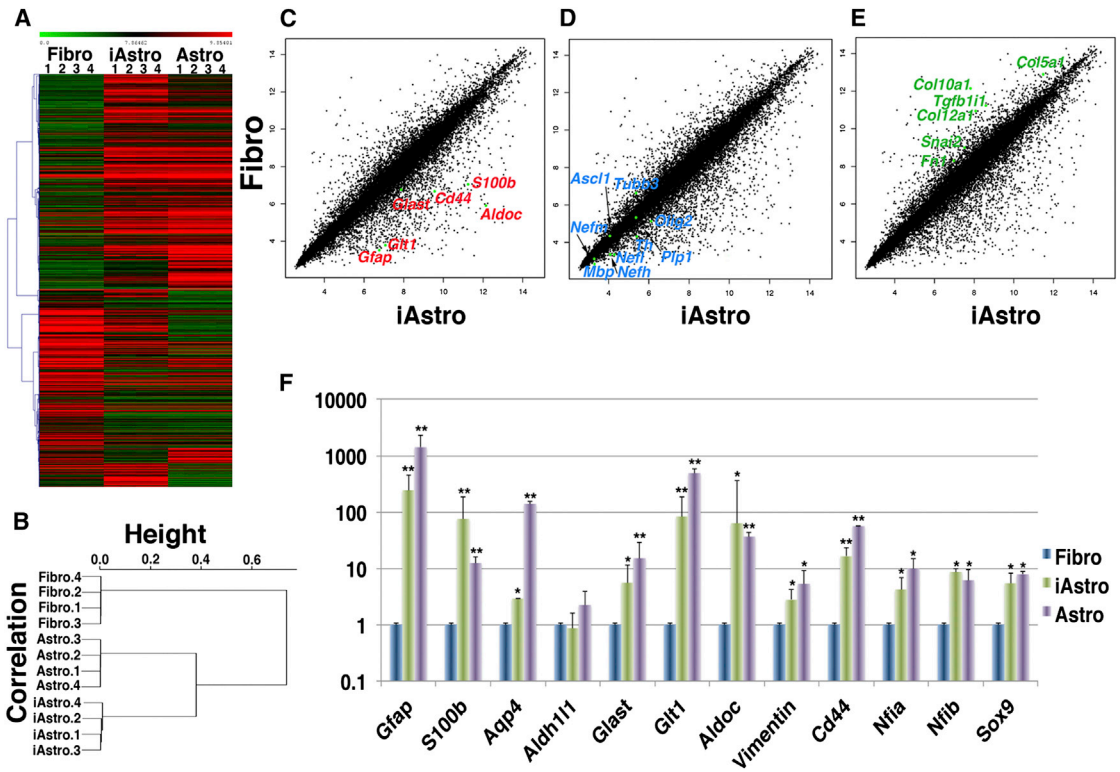

Figure 2. Transcriptional Profiling of iAstrocytes

(A) Microarray analysis comparison among noninfected MEFs (Fibro), induced astrocytes (iAstro), and primary cortical astrocytes (Astro).

(B) Hierarchical clustering of the analyzed samples shows a strong degree of correlation between iAstro and primary astrocytes.

(C–E) Scatterplot comparison between fibroblasts and iAstro shows that most of the astrocytic markers are increased in reprogrammed cells (C), whereas other neural markers are unaltered (D) and some fibroblasts markers are silenced (E).

(F) Real-time RT-PCR analysis confirms that the expression of most astrocytic markers is comparable between iAstro and primary astrocytes.

Data are expressed as means ± SEM. *$p < 0.05$; **$p < 0.01$. Three independent experiments are represented in (F).

iAstrocytes Resemble Native Brain Astrocytes in Global Gene-Expression Profiling

To fully investigate the reprogrammed state of iAstrocytes, we compared the global gene-expression pattern of MEFs, iAstrocytes, as well as neonatal primary brain astrocytes by microarray analysis. Considering that, during embryonic development, GFAP is also expressed in NSCs and neural precursors (Rowitch and Kriegstein, 2010), we could not use the hGFAP-Cre;ROSA26-stop-flox-YFP mouse to derive primary astrocytes. Thus, to avoid possible contamination of YFP+/GFAP− cells due to the transient embryonic GFAP expression, we opted to derive astrocyte primary cultures from the hGFAP-Cre mice that were subsequently infected with the TET-O-FUW-flox-stop-flox-GFP construct in order to timely activate the reporter in well-differentiated astrocytes. On the same line, to avoid any contamination due to hGFAP promoter leakiness (Niu et al., 2013; data not shown), iAstrocytes were reprogrammed from a GFP-negative-sorted MEF population. The heatmap comparison between MEFs, iAstrocytes, and native brain astrocytes clearly showed that the iAstrocyte gene-expression signature was close to that of primary astrocytes, although some clusters of genes were still diverging (Figure 2A). The unbiased hierarchical clustering also confirmed that iAstrocytes transcriptional pattern segregated significantly closer to primary brain astrocytes than to MEFs (Figure 2B). When our attention was focused on the comparison of specific set of genes between MEFs and iAstrocytes, we observed that most of the astrocyte-specific genes were strongly upregulated in iAstrocytes (Figure 2C), whereas, at the same time, genes strictly associated with other neural lineages did not show evident upregulation (Figure 2D). Noteworthy, many fibroblast-specific molecular markers resulted evidently downregulated after astrocyte reprogramming as shown in Figure 2E. Finally, to confirm microarray data, we performed an extensive qRT-PCR analysis for several known astrocyte markers and confirmed that the vast majority of them were significantly activated in

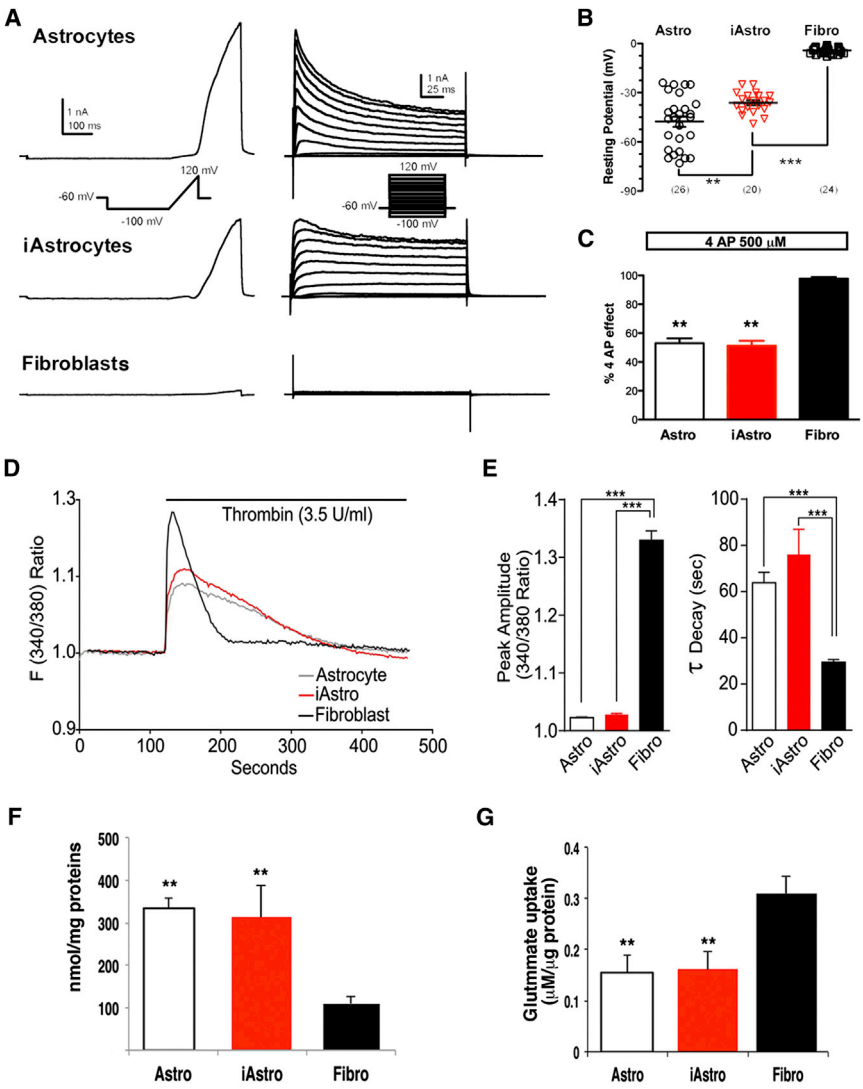

Figure 3. Functional Characterization of Induced Astrocytes

(A) Representative traces of ionic currents evoked in mouse-cultured cortical astrocytes (Astro), iAstrocytes (iAstro), and fibroblasts (Fibro) using a ramp (left) and voltage-step protocol (right). The stimulation protocols are depicted as insets and described in Experimental Procedures.

(B) Graph of resting membrane potential values for the three cell types recorded before the membrane current activation.

(C) Percentage of ramp current decrease measured at +100 mV by application of 4-AP (500 μM) in iAstrocytes, cortical astrocytes, and fibroblasts.

(D) Representative Fura-2 responses triggered by thrombin (3.5 U/ml) application over time in astrocytes (gray trace), iAstrocytes (red trace), and fibroblasts (black trace).

(E) The peak amplitudes of Fura-2 responses and the τ values of Ca^{2+} decay are shown as means ± SEM of three independent experiments ($n > 50$).

(F and G) Glutamate uptake assay. [^{3}H]L-glutamate cell content (F) and corresponding glutamate levels in the medium (G). $^{**}p < 0.01$; $^{***}p < 0.001$.

Data are expressed as means ± SEM. Five cells recorded in three independent experiments are represented in (C) and (E). Three independent experiments are represented in (F) and (G).

iAstrocytes with expression levels roughly comparable between iAstrocytes and native brain astrocytes (Figure 2F). Moreover, we found that even the three astroglial reprograming factors ABS9 were endogenously upregulated in iAstrocytes (Figure 2F), confirming a global activation of the astrocytic transcriptional program.

iAstrocytes Share Critical Functions with Native Brain Astrocytes

We next sought to determine whether iAstrocytes were endowed with functional properties consistent with their new reprogrammed cell state. To address this point, iAstrocytes electrophysiological properties were investigated by patch-clamp recording. Given that MEFs are a quite heterogeneous cell population where some neural progenitor contaminants cannot be excluded, we opted for a more-homogeneous source of fibroblasts collected from the isolated mouse postnatal dermis for the following experiments of cell reprogramming. Initially, we compared fibroblasts, iAstrocytes, and native brain astrocytes for they ability to generate K^+ currents upon voltage stimulation. Ramp currents evoked in mouse cortical astrocytes and iAstrocytes showed an outwardly rectifying profile at potentials more positive than −40 mV (Figure 3A, left panel). This observation is in agreement with previous data indicating that whereas rodent astrocytes in situ display a large inwardly rectifying K^+ conductance, which is developmentally regulated (Kressin et al., 1995; Bordey and Sontheimer, 1997; Zhou et al., 2006), primary cultured astroglial cells express only large outward-rectifying K^+ currents (Bevan and Raff, 1985; Ferroni et al., 1995). By contrast, fibroblasts exhibit a small, linear membrane conductance in the whole range of potentials tested, denoting the high membrane resistance and the lack of any activation of voltage-gated

channels (Figure 3A, left panel). Upon application of a voltage-step protocol, typical outward K^+ currents characterized by rapid activation kinetics, partial slow inactivation, and a sustained component were evoked in astrocytes and iAstrocytes, but not in fibroblasts (Figure 3A, right panels). Currents evoked in iAstrocytes displayed a less-prominent inactivation phase compared to brain astrocytes, a result that could be ascribed to a different state of cell development (Bordey and Sontheimer, 1997). The presence of voltage-gated K^+ currents in iAstrocytes was accompanied by a change in resting membrane potential (RMP) that became significantly more negative than that of fibroblasts but still slightly more positive than the RMP measured in primary cortical astrocytes (Figure 3B; -47.69 ± 3.71 mV, n = 26; iAstro: -36.15 ± 1.44, n = 20; fibroblasts: -4.33 ± 0.39, n = 24). Consistent with the notion that the outward current was a K^+ conductance, the voltage-gated currents in both astrocytes and iAstrocytes were similarly depressed by about 50% by the K^+ channel blocker 4-aminopyridine (Figure 3C; 500 μM; astrocytes: 53% ± 3.37%, n = 4; iAstrocytes: 51.25% ± 3.47%, n = 5; fibroblasts: 97.8% ± 1.09%, n = 5) that was previously reported to inhibit by the same extent voltage-gated K^+ channels in cultured astrocytes (Bordey and Sontheimer, 1997). We also scrutinized iAstrocytes for their capacity to generate intracellular calcium waves after thrombin application. There is evidence, in fact, that astrocytes express a protease-activated receptor (PAR), which is a G-protein-coupled receptor activated by thrombin (Coughlin, 2000). In cultured astrocytes, PAR activation by thrombin leads to robust Ca^{2+} mobilization involving inositol-triphosphate-dependent intracellular Ca^{2+} release, which promotes Ca^{2+} entry (Ubl and Reiser, 1997). PAR can be activated by thrombin also in fibroblasts but generates faster Ca^{2+} dynamics (Tanaka et al., 2003; Jeng et al., 2004; Rössler and Thiel, 2009). We then performed Ca^{2+} imaging experiments using Fura-2/AM as ratiometric Ca^{2+} indicator in astrocytes, fibroblasts, and iAstrocytes by activating Ca^{2+} mobilization after application of human thrombin (3.5 U/ml). In all experimental groups, thrombin evoked a rising of intracellular Ca^{2+} but with substantial main differences between fibroblasts and either astrocytes or iAstrocytes (Figure 3D). Whereas the Ca^{2+} peak was significantly higher and the τ of Ca^{2+} decay was faster in fibroblasts, astrocytes and iAstrocytes displayed Ca^{2+} peaks of lower amplitude and slower kinetics (Figure 3E). These results, together with the previous electrophysiological data, suggest that iAstrocytes and native astrocytes share critical functions that are undetectable in the original population of primary fibroblasts before their genetic reprogramming. Finally, we tested whether iAstrocytes exhibit the capability of glutamate uptake, another critical property of brain astroglial cells (Anderson and Swanson 2000). To quantitatively test glutamate uptake, fibroblasts, iAstrocytes, and primary brain astrocytes were cultured in a medium containing [^{3}H]L-glutamate, and the radioactivity in cellular extracts was quantified (n = 6). As shown in Figure 3F, iAstrocytes and brain astrocytes incorporated similar levels of radioactivity that were significantly higher than those present in cell lysates of fibroblasts. This result was corroborated by the observation that the amount of glutamate remaining in the bathing medium measured by an enzymatic determination method was significantly lower in the astroglial cells with respect to the fibroblasts (n = 6; Figure 3G). These results indicate that both astroglial cell types were similarly proficient in incorporating glutamate. These data confirm that iAstrocytes develop an intrinsic ability to uptake glutamate, demonstrating the full functionality of the glutamate transporters. These findings indicate that both native astroglial cells and iAstrocytes exhibit comparable capacity of glutamate uptake, which is much lower in native fibroblasts. Altogether, these assays denote that iAstrocytes possess functional properties of primary astrocytes that are absent in the original population of primary fibroblasts before their genetic reprogramming.

iAstrocytes Undergo an Activated State when Exposed to Cytokine Stimulation

Astrocytes are crucial for their role in the physiological homeostasis of the CNS, but they are also known to take part in the inflammatory response (Barres, 2008; Sofroniew and Vinters, 2010; Sofroniew, 2014). Indeed, astrocytes retain the ability to shift from a quiescent to an activated state following the exposure to cytokines (Ridet et al., 1997). Cytokines are key mediators of the inflammatory response in the CNS, resulting, among others, in an increase of GFAP-positive cells as well as in the activation of the NF-kB pathway (Buffo et al., 2010; Moynagh, 2005). To test the competence in responding to cytokine stimulation, we treated dermal neonatal-derived iAstrocytes with interleukin-1 (IL-1) for 24 hr and looked at the effects on cell proliferation and the NF-kB molecular pathway. Consistent with the known astrocyte behavior (Ridet et al., 1997; Buffo et al., 2010), IL-1 exposure resulted in an increased number of cells positive for GFAP, but not for S100B, a protein which is not associated with the astrocyte-activation process (Figures 4A–4D). On the same line, the transcriptional analysis revealed that IL-1 treatment in iAstrocytes induced an increase in *Gfap* expression and a positive feedback of cytokine expression as indicated by the increase of *Il1* and interleukin-6 transcripts. iAstrocytes responded to cytokine stimulus also by activating the NF-kB pathway, as demonstrated by the significantly increased expression of the molecular components *Nfkb1*, *Nfkb2*, and *Nfkbia* (Figure 4E). These results stand as a proof of principle

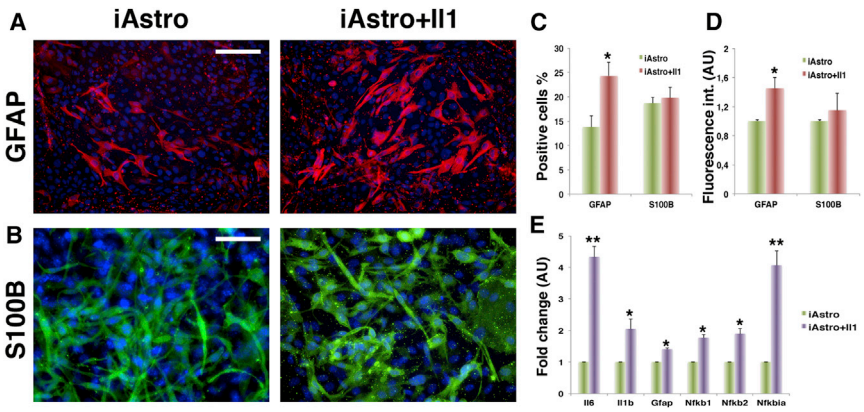

Figure 4. Activation of iAstrocytes by Cytokines

(A and B) Immunocytochemical analysis shows that GFAP expression (A) is higher in interleukin-1-stimulated (iAstro+Il1) than in untreated iAstrocytes (iAstro), whereas S100B expression (B) is not affected.

(C and D) Quantification of GFAP- and S100B-positive cells (C) and staining intensity (D) in control and Il1-treated cells. AU, arbitrary units.

(E) Real-time RT-PCR analysis shows that NF-kB pathway is significantly activated in induced astrocytes after Il1 treatment. Cells nuclei are stained with DAPI.

Data are expressed as means ± SEM. *$p < 0.05$; **$p < 0.01$. The scale bar represents 60 μm (A) and 30 μm (B). Four independent experiments are represented in (C)–(E).

showing iAstrocytes to be able to respond to external stimuli and adapt their behavior to the surrounding environmental conditions.

We finally asked whether the reprogrammed state of iAstrocytes remains stable after transplantation in vivo. To this aim, we transplanted YFP-labeled iAstrocytes into the brain parenchyma of neonatal mice and examined the grafted brains 2 weeks after. Immunohistochemistry revealed the presence of GFAP/GFP and S100/GFP double-positive cells (Figures S5A–S5G), indicating that iAstrocytes are able to survive and differentiate in the host brain over an extensive time period. Grafted iAstrocytes organized in islands in the transplanted site, and their spreading in the host tissue appeared limited (Figures S5A and S5H). This is not surprising, considering that native astrocytes are well known to release high amounts of extracellular matrix (ECM) components, which create a barrier to cell spreading (Dityatev and Rusakov, 2011). In accordance with this hypothesis, we found that grafted iAstrocytes are surrounded by a rich ECM that confined the transplanted cells from the host tissue (Figures S5H–S5J).

NFIA, NFIB, and SOX9 Are Able to Induce an Astrocytic Phenotype in Human Fibroblasts

Considering the huge implications of the potential generation of human iAstrocytes, we decided to test the ABS9-reprogramming cocktail on human cells. Indeed, NFIA, NFIB, and SOX9 are expressed in human fetal astrocytes (Mense et al., 2006), and recently, NFI proteins have been found among the transcription factors enriched in human fetal astrocytes (Malik et al., 2014). Therefore, considering that human reprogramming dynamics are substantially slower, we infected human neonatal fibroblasts with ABS9 cocktail, keeping them activated for 3 weeks. Surprisingly, the following immunocytochemical analysis showed that a small fraction of cells (~2%) were coexpressing GFAP and S100B with a typical pattern as normally detected in immature astrocytes, whereas no signal was revealed in not-infected control (Figures 5A–5D). This experimental evidence gives a clear proof of principle that the direct conversion of human fibroblasts into iAstrocytes is possible, thus opening opportunities in the field of human cell reprogramming.

DISCUSSION

Altogether, this study demonstrates the possibility to convert adult somatic cells such as dermal fibroblasts into astroglial-like cells through the overexpression of only a minimal set of the three factors NFIA, NFIB, and SOX9. These results, together with previous reports, demonstrate the possibility to reprogram mesodermal cells directly into any of the three neuronal lineages including neurons (Vierbuchen et al., 2010), oligodendrocytes (Najm et al., 2013; Yang et al., 2013), and astrocytes (this report).

Our findings are corroborated by a previous report, showing that NFIA and SOX9 associate in a protein complex during the initial phases of gliogenesis in early development (Kang et al., 2012). This study demonstrated that NFIA and SOX9 form a transcriptional regulatory module, which is necessary for the timely initiation of the gliogenic process in the spinal cord anlage. Herein, we provided evidence that these factors can even promote and sustain a global astroglial gene program in mesodermal cells and activate the expression of mature astrocytes markers such as S100B, GLT1, ALDOC, and CD44 necessary to acquire cardinal functional properties of mature astrocytes. In support of these findings, the ABS9 gene combination is

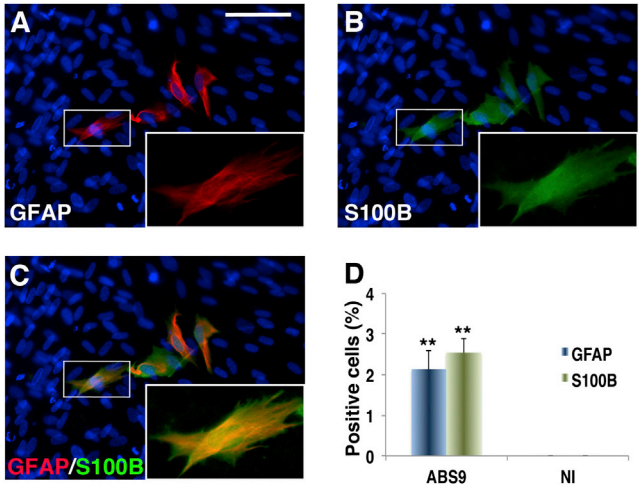

Figure 5. Conversion of Human Fibroblasts into iAstrocytes

(A–C) Immunocytochemical analysis of GFAP and S100B in human neonatal fibroblasts reprogrammed with NFIA, NFIB, and SOX9 (ABS9) for 3 weeks. The insets show higher magnification of typical GFAP or S100B staining signals.

(D) Quantification of GFAP- and S100B-positive cells in ABS9 or NI cells. Cells nuclei are stained with DAPI.

Data are expressed as means ± SEM. **p < 0.01. The scale bar represents 50 μm. Three independent experiments are represented in (D).

capable of suppressing the neuronal fate of early neural progenitors while activating the expression of astroglial markers.

iAstrocytes do not show any particular regional identity in agreement with the pan-astroglial expression of all the three reprogramming TFs. We can, however, speculate that the addition of a fourth factor could be sufficient for imposing a regional specification to the iAstrocytes that may associate with the acquisition of supplementary and region-specific functions (Pang et al., 2011; Yoo et al., 2011). In the final part of the present work, we also provided a proof of principle that NFIA, NFIB, and SOX9 are able to activate an astroglial program even in human neonatal fibroblasts. Further experiments are needed to prove the functional similarity to human astrocytes and also to increase the low efficiency of conversion showed by human fibroblasts. Nonetheless, these results lay the ground for the future generation of human iAstrocytes. If accomplished, these results would be of great interest for biomedical applications. In fact, recent findings have disclosed a previously unknown role of the astrocytic compartment in the genesis and progression of an increasing number of neurological disorders (Lioy et al., 2011; Di Giorgio et al., 2008; Coulter and Eid, 2012; McGann et al., 2012; Di Malta et al., 2012). Thus, the opportunity to have a fast way to generate high numbers of human astrocytes from patients will provide an extremely versatile and informative cellular system for investigating the pathophysiological processes in these cells. In addition, transplantation of astrocytes has been found beneficial in several disorders, including Parkinson's disease and ALS (Proschel et al., 2014; Lepore et al., 2008). This approach does not aim at replacing a lost neuronal circuit but at delaying and restraining neuronal dysfunctions and therefore has less constrains and multiple potential applications. Nowadays, the main perspective for an astrocyte cell-replacement therapy is linked to the employment of iPSCs that still share a lot of limitations due to their intrinsic capacity to generate tumors (Roy et al., 2006; Amariglio et al., 2009). To our knowledge, this is the first evidence that astrocyte-like cells can be derived from fibroblasts by entirely skipping the iPSC generation. Therefore, our findings represent a crucial step for the potential future application of iAstrocytes in human disease biology and therapy.

EXPERIMENTAL PROCEDURES

Cell Culture

MEFs were isolated from E14.5 wild-type or hGFAP-Cre;ROSA26-flox-stop-flox-YFP mice embryos. Only forelimbs and forelegs were taken, and the tissue was manually dissociated and incubated in 0.25% trypsin (Sigma) for 10–15 min. Cells from each embryo were plated onto a 15 cm tissue culture dish in MEF medium (Dulbecco's modified Eagle's medium [Invitrogen], containing 10% fetal bovine serum [Hyclone], β-mercaptoethanol [Sigma], nonessential amino acids [Invitrogen], sodium pyruvate, and penicillin/streptomycin [Invitrogen]). In all experiments, cells were not passaged more than four times. Postnatal fibroblasts were isolated from dermis. Pups were sacrificed and skinned, and dermis was isolated by overnight 0.25% trypsin treatment. Dermis was then mechanically minced and dissociated with 0.25% trypsin for 10–15 min, placed on culture dishes, and grown in MEF media. IL-1 (R&D Systems) 10 ng/ml was added for 24 hr to induce iAstrocytes stimulation. Human neonatal foreskin fibroblasts (ATCC; PCS-201-010) were grown in MEF medium.

Molecular Cloning and Viral Infection

cDNAs for the astrocytic transcription factors were cloned into lentiviral vectors under the control of the tetracycline operator. Replication-incompetent, VSVg-coated lentiviral particles were packaged in 293T cells. MEFs or postnatal mouse fibroblasts were infected in MEF medium using each virus at 25 multiplicity of infection. Sixteen to twenty hours after infection, cells were switched into fresh MEF media containing doxycycline (2 μg/ml; Sigma). After 24 hr, doxycycline was added to the medium. The medium was changed every 2 or 3 days for further 12–16 days.

Cell Sorting and Microarray Analysis

GFAP-YFP-positive iAstrocytes were sorted using the cell sorter FACSVantage SE. DiVa (Becton Dickinson) and RNA was extracted with RNeasy Plus Mini Kit (QIAGEN). GeneChip Mouse Genome

430A 2.0 Arrays (Affymetrix) were hybridized with cRNA. Microarray data were preprocessed using Bioconductor package Affy (Gautier et al., 2004) and normalized using robust multiarray average method (Irizarry et al., 2003). Differentially expressed genes among iAstrocytes, primary postnatal cortical astrocytes, and MEFs were identified through a one-way ANOVA using one factor with three levels (iAstro/primary postnatal cortical astrocyte [PPCA]/MEF). p values were corrected for multiplicity according to the Benjamini-Hochberg procedure (false discovery rate [FDR]; Benjamini and Hochberg, 1995). The threshold used for the FDR was 0.05. The differentially expressed genes between conditions (iAstro versus MEF, PPCA versus MEF, and iAstro versus PPCA) were analyzed using the post hoc Tukey multiple comparisons test (p value < 0.05). Results were further filtered by change magnitude (|fold change| $\geq$ 2), and the differentially expressed genes were classified on the basis of the comparison tests they have passed.

Electrophysiology

After 12 days of reprograming, cells were plated at density of 1 or 2 × 10^4 onto 33 mm Petri dishes after trypsin-EDTA enzymatic dispersion and electrophysiological recordings were made 2–4 days later. Membrane currents were recorded using the whole-cell configuration of the patch-clamp technique, as previously described (Ferroni et al., 1995; Valente et al., 2011). Patch pipettes prepared from thin-walled borosilicate glass capillaries (Hilgenberg) were pulled and fire-polished to have a tip resistance of 3 or 4 MΩ when filled with standard internal solution. Data were sampled at 10 kHz (double EPC-10 amplifier with Pulse software; HEKA Electronic) and low-pass filtered at 3 kHz for analysis (Fitmaster 2.73; HEKA). The series resistance was usually <10 MΩ and to minimize voltage errors was compensated to 60%–80%. Recordings with leak currents >100 pA were discarded. All measurements were performed at room temperature (20°C–24°C). The protocols of voltage stimulation consisted of either a repetitive protocol that, from the holding potential (V_h) of −60 mV, stepped the membrane potential to −100 mV for 200 ms before a 100 ms long depolarizing ramp to +120 mV or a voltage-step family with 200 ms steps from 100 mV to +120 mV in 20 mV increments from the V_h of −60 mV. The interval between each pulse in both protocols was 10 s. Membrane capacitances and current values recorded at the end of the linear ramp were used to calculate current densities. The resting membrane potential was measured 2 min after establishing the whole-cell recording configuration using the amplifier analog circuit. Recordings were made by superfusing the clamped cell with a standard bath saline solution containing (in mM): 140 NaCl, 4 KCl, 2 $MgCl_2$, 2 $CaCl_2$, 10 HEPES, 5 glucose (pH 7.4) with NaOH, and osmolality adjusted to 315 mOsm kg^{-1} with mannitol. The intracellular pipette solution contained (in mM): 144 KCl, 2 $MgCl_2$, 5 EGTA, 10 HEPES (pH 7.2) with KOH, and osmolality of 300 mOsm kg^{-1} with mannitol. The extracellular solution was applied by gravity-driven microperfusion system at flow rate of about 200 μl/min located near (≈100 μm) the cell under study.

Calcium Imaging

Astrocytes, iAstrocytes, and fibroblasts were loaded with Fura-2, AM (5 mM; Molecular Probes) for 1 hr at 37°C, 5% CO_2 in culture medium. Coverslips were mounted on the stage of an IX-71 inverted microscope (Olympus) equipped with a monochromator (Polychrome V; TILL Photonics). Cells were imaged in in standard bath saline solution containing (in mM): 2 $CaCl_2$, 140 NaCl, 1 $MgCl_2$, 10 HEPES, 4 KCl, 10 glucose (pH 7.3), and 300 mOsm kg^{-1} by using a cooled charge-coupled device camera (ANDOR; iXon 897) and sampling at 0.5 Hz with a 40 objective (0.95 numerical aperture). After 2 min baseline, 3.5 U/ml human thrombin was added to the bath. The offline analysis of the fluorescent intensities ratio at 340 and 380 nm was performed with the TILL-vision software and normalized to the baseline.

ACCESSION NUMBERS

Microarray data have been deposited with Gene Expression Omnibus accession number GSE59018.

SUPPLEMENTAL INFORMATION

Supplemental Information includes Supplemental Experimental Procedures, five figures, and one table and can be found with this article online at http://dx.doi.org/10.1016/j.stemcr.2014.12.002.

AUTHOR CONTRIBUTIONS

M.C., C.S., and V.B. planned the experiments; M.C., S.G., P.V., G.L., A.C., G.C., A.S., R.B., and L.M. performed research and acquired data; M.C., S.G., P.V., G.L., A.C., S.F., C.S., F.B., and V.B. analyzed data and wrote the respective methods and results; M.C. and V.B. supervised the project; and M.C and V.B. wrote the paper.

ACKNOWLEDGMENTS

We thank A. Fasciani and D. Brina for technical help and A. Buffo, G. Martino, M. Bacigaluppi, G. Messina, C. Farina, and M. Colombo for helpful suggestions and reagent sharing. This study was supported by Italian Ministry of Health, European Research Council (ERC) Advanced grant ReproPARK, CoEN Initiative (to V.B.); Telethon-GGP13033 and Fondazione Istituto Italiano di Tecnologia (to F.B.); EC FP7-HEALTH-2013-INNOVATION integrating project "Desire" (to F.B. and V.B.); and FIRB 2013 grant from the Italian Ministry of University and Research (to M.C. and C.S.).

Received: June 24, 2014
Revised: November 28, 2014
Accepted: December 1, 2014
Published: December 31, 2014

REFERENCES

Amariglio, N., Hirshberg, A., Scheithauer, B.W., Cohen, Y., Loewenthal, R., Trakhtenbrot, L., Paz, N., Koren-Michowitz, M., Waldman, D., Leider-Trejo, L., et al. (2009). Donor-derived brain tumor following neural stem cell transplantation in an ataxia telangiectasia patient. PLoS Med. *6*, e1000029.

Anderson, C.M., and Swanson, R.A. (2000). Astrocyte glutamate transport: review of properties, regulation, and physiological functions. Glia *32*, 1–14.

Barres, B.A. (2008). The mystery and magic of glia: a perspective on their roles in health and disease. Neuron *60*, 430–440.

Benjamini, Y., and Hochberg, Y. (1995). Controlling the false discovery rate: a practical and powerful approach to multiple testing. J. R. Stat. Soc., B *57*, 289–300.

Bevan, S., and Raff, M. (1985). Voltage-dependent potassium currents in cultured astrocytes. Nature *315*, 229–232.

Bordey, A., and Sontheimer, H. (1997). Postnatal development of ionic currents in rat hippocampal astrocytes in situ. J. Neurophysiol. *78*, 461–477.

Buffo, A., Rolando, C., and Ceruti, S. (2010). Astrocytes in the damaged brain: molecular and cellular insights into their reactive response and healing potential. Biochem. Pharmacol. *79*, 77–89.

Cahoy, J.D., Emery, B., Kaushal, A., Foo, L.C., Zamanian, J.L., Christopherson, K.S., Xing, Y., Lubischer, J.L., Krieg, P.A., Krupenko, S.A., et al. (2008). A transcriptome database for astrocytes, neurons, and oligodendrocytes: a new resource for understanding brain development and function. J. Neurosci. *28*, 264–278.

Caiazzo, M., Dell'Anno, M.T., Dvoretskova, E., Lazarevic, D., Taverna, S., Leo, D., Sotnikova, T.D., Menegon, A., Roncaglia, P., Colciago, G., et al. (2011). Direct generation of functional dopaminergic neurons from mouse and human fibroblasts. Nature *476*, 224–227.

Chambers, S.M., and Studer, L. (2011). Cell fate plug and play: direct reprogramming and induced pluripotency. Cell *145*, 827–830.

Coughlin, S.R. (2000). Thrombin signalling and protease-activated receptors. Nature *407*, 258–264.

Coulter, D.A., and Eid, T. (2012). Astrocytic regulation of glutamate homeostasis in epilepsy. Glia *60*, 1215–1226.

Deneen, B., Ho, R., Lukaszewicz, A., Hochstim, C.J., Gronostajski, R.M., and Anderson, D.J. (2006). The transcription factor NFIA controls the onset of gliogenesis in the developing spinal cord. Neuron *52*, 953–968.

Di Giorgio, F.P., Boulting, G.L., Bobrowicz, S., and Eggan, K.C. (2008). Human embryonic stem cell-derived motor neurons are sensitive to the toxic effect of glial cells carrying an ALS-causing mutation. Cell Stem Cell *3*, 637–648.

Di Malta, C., Fryer, J.D., Settembre, C., and Ballabio, A. (2012). Astrocyte dysfunction triggers neurodegeneration in a lysosomal storage disorder. Proc. Natl. Acad. Sci. USA *109*, E2334–E2342.

Dityatev, A., and Rusakov, D.A. (2011). Molecular signals of plasticity at the tetrapartite synapse. Curr. Opin. Neurobiol. *21*, 353–359.

Doyle, J.P., Dougherty, J.D., Heiman, M., Schmidt, E.F., Stevens, T.R., Ma, G., Bupp, S., Shrestha, P., Shah, R.D., Doughty, M.L., et al. (2008). Application of a translational profiling approach for the comparative analysis of CNS cell types. Cell *135*, 749–762.

Emdad, L., D'Souza, S.L., Kothari, H.P., Qadeer, Z.A., and Germano, I.M. (2012). Efficient differentiation of human embryonic and induced pluripotent stem cells into functional astrocytes. Stem Cells Dev. *21*, 404–410.

Ferroni, S., Marchini, C., Schubert, P., and Rapisarda, C. (1995). Two distinct inwardly rectifying conductances are expressed in long term dibutyryl-cyclic-AMP treated rat cultured cortical astrocytes. FEBS Lett. *367*, 319–325.

Gautier, L., Cope, L., Bolstad, B.M., and Irizarry, R.A. (2004). affy–analysis of Affymetrix GeneChip data at the probe level. Bioinformatics *20*, 307–315.

Graf, T., and Enver, T. (2009). Forcing cells to change lineages. Nature *462*, 587–594.

Huang, P., He, Z., Ji, S., Sun, H., Xiang, D., Liu, C., Hu, Y., Wang, X., and Hui, L. (2011). Induction of functional hepatocyte-like cells from mouse fibroblasts by defined factors. Nature *475*, 386–389.

Ieda, M., Fu, J.D., Delgado-Olguin, P., Vedantham, V., Hayashi, Y., Bruneau, B.G., and Srivastava, D. (2010). Direct reprogramming of fibroblasts into functional cardiomyocytes by defined factors. Cell *142*, 375–386.

Irizarry, R.A., Hobbs, B., Collin, F., Beazer-Barclay, Y.D., Antonellis, K.J., Scherf, U., and Speed, T.P. (2003). Exploration, normalization, and summaries of high density oligonucleotide array probe level data. Biostatistics *4*, 249–264.

Jeng, J.H., Chan, C.P., Wu, H.L., Ho, Y.S., Lee, J.J., Liao, C.H., Chang, Y.K., Chang, H.H., Chen, Y.J., Perng, P.J., and Chang, M.C. (2004). Protease-activated receptor-1-induced calcium signaling in gingival fibroblasts is mediated by sarcoplasmic reticulum calcium release and extracellular calcium influx. Cell. Signal. *16*, 731–740.

Juopperi, T.A., Kim, W.R., Chiang, C.H., Yu, H., Margolis, R.L., Ross, C.A., Ming, G.L., and Song, H. (2012). Astrocytes generated from patient induced pluripotent stem cells recapitulate features of Huntington's disease patient cells. Mol. Brain *5*, 17.

Kang, P., Lee, H.K., Glasgow, S.M., Finley, M., Donti, T., Gaber, Z.B., Graham, B.H., Foster, A.E., Novitch, B.G., Gronostajski, R.M., and Deneen, B. (2012). Sox9 and NFIA coordinate a transcriptional regulatory cascade during the initiation of gliogenesis. Neuron *74*, 79–94.

Kim, J.H., Auerbach, J.M., Rodríguez-Gómez, J.A., Velasco, I., Gavin, D., Lumelsky, N., Lee, S.H., Nguyen, J., Sánchez-Pernaute, R., Bankiewicz, K., and McKay, R. (2002). Dopamine neurons derived from embryonic stem cells function in an animal model of Parkinson's disease. Nature *418*, 50–56.

Krencik, R., Weick, J.P., Liu, Y., Zhang, Z.J., and Zhang, S.C. (2011). Specification of transplantable astroglial subtypes from human pluripotent stem cells. Nat. Biotechnol. *29*, 528–534.

Kressin, K., Kuprijanova, E., Jabs, R., Seifert, G., and Steinhäuser, C. (1995). Developmental regulation of Na+ and K+ conductances in glial cells of mouse hippocampal brain slices. Glia *15*, 173–187.

Lepore, A.C., Rauck, B., Dejea, C., Pardo, A.C., Rao, M.S., Rothstein, J.D., and Maragakis, N.J. (2008). Focal transplantation-based astrocyte replacement is neuroprotective in a model of motor neuron disease. Nat. Neurosci. *11*, 1294–1301.

Lioy, D.T., Garg, S.K., Monaghan, C.E., Raber, J., Foust, K.D., Kaspar, B.K., Hirrlinger, P.G., Kirchhoff, F., Bissonnette, J.M., Ballas, N., and Mandel, G. (2011). A role for glia in the progression of Rett's syndrome. Nature *475*, 497–500.

Liu, M.L., Zang, T., Zou, Y., Chang, J.C., Gibson, J.R., Huber, K.M., and Zhang, C.L. (2013). Small molecules enable neurogenin 2 to

efficiently convert human fibroblasts into cholinergic neurons. Nat. Commun. *4*, 2183.

Lovatt, D., Sonnewald, U., Waagepetersen, H.S., Schousboe, A., He, W., Lin, J.H.C., Han, X., Takano, T., Wang, S., Sim, F.J., et al. (2007). The transcriptome and metabolic gene signature of protoplasmic astrocytes in the adult murine cortex. J. Neurosci. *27*, 12255–12266.

Malik, N., Wang, X., Shah, S., Efthymiou, A.G., Yan, B., Heman-Ackah, S., Zhan, M., and Rao, M. (2014). Comparison of the gene expression profiles of human fetal cortical astrocytes with pluripotent stem cell derived neural stem cells identifies human astrocyte markers and signaling pathways and transcription factors active in human astrocytes. PLoS ONE *9*, e96139.

McGann, J.C., Lioy, D.T., and Mandel, G. (2012). Astrocytes conspire with neurons during progression of neurological disease. Curr. Opin. Neurobiol. *22*, 850–858.

Mense, S.M., Sengupta, A., Lan, C., Zhou, M., Bentsman, G., Volsky, D.J., Whyatt, R.M., Perera, F.P., and Zhang, L. (2006). The common insecticides cyfluthrin and chlorpyrifos alter the expression of a subset of genes with diverse functions in primary human astrocytes. Toxicol. Sci. *93*, 125–135.

Molofsky, A.V., Krencik, R., Ullian, E.M., Tsai, H.H., Deneen, B., Richardson, W.D., Barres, B.A., and Rowitch, D.H. (2012). Astrocytes and disease: a neurodevelopmental perspective. Genes Dev. *26*, 891–907.

Moynagh, P.N. (2005). The interleukin-1 signalling pathway in astrocytes: a key contributor to inflammation in the brain. J. Anat. *207*, 265–269.

Najm, F.J., Lager, A.M., Zaremba, A., Wyatt, K., Caprariello, A.V., Factor, D.C., Karl, R.T., Maeda, T., Miller, R.H., and Tesar, P.J. (2013). Transcription factor-mediated reprogramming of fibroblasts to expandable, myelinogenic oligodendrocyte progenitor cells. Nat. Biotechnol. *31*, 426–433.

Niu, W., Zang, T., Zou, Y., Fang, S., Smith, D.K., Bachoo, R., and Zhang, C.L. (2013). In vivo reprogramming of astrocytes to neuroblasts in the adult brain. Nat. Cell Biol. *15*, 1164–1175.

Pang, Z.P., Yang, N., Vierbuchen, T., Ostermeier, A., Fuentes, D.R., Yang, T.Q., Citri, A., Sebastiano, V., Marro, S., Südhof, T.C., and Wernig, M. (2011). Induction of human neuronal cells by defined transcription factors. Nature *476*, 220–223.

Pfisterer, U., Kirkeby, A., Torper, O., Wood, J., Nelander, J., Dufour, A., Björklund, A., Lindvall, O., Jakobsson, J., and Parmar, M. (2011). Direct conversion of human fibroblasts to dopaminergic neurons. Proc. Natl. Acad. Sci. USA *108*, 10343–10348.

Pihlaja, R., Koistinaho, J., Malm, T., Sikkilä, H., Vainio, S., and Koistinaho, M. (2008). Transplanted astrocytes internalize deposited beta-amyloid peptides in a transgenic mouse model of Alzheimer's disease. Glia *56*, 154–163.

Proschel, C., Stripay, J.L., Shih, C.H., Munger, J.C., and Noble, M.D. (2014). Delayed transplantation of precursor cell-derived astrocytes provides multiple benefits in a rat model of Parkinsons. EMBO Mol. Med. *6*, 504–518.

Ridet, J.L., Malhotra, S.K., Privat, A., and Gage, F.H. (1997). Reactive astrocytes: cellular and molecular cues to biological function. Trends Neurosci. *20*, 570–577.

Rössler, O.G., and Thiel, G. (2009). Thrombin induces Egr-1 expression in fibroblasts involving elevation of the intracellular Ca2+ concentration, phosphorylation of ERK and activation of ternary complex factor. BMC Mol. Biol. *10*, 40.

Rowitch, D.H. (2004). Glial specification in the vertebrate neural tube. Nat. Rev. Neurosci. *5*, 409–419.

Rowitch, D.H., and Kriegstein, A.R. (2010). Developmental genetics of vertebrate glial-cell specification. Nature *468*, 214–222.

Roy, N.S., Cleren, C., Singh, S.K., Yang, L., Beal, M.F., and Goldman, S.A. (2006). Functional engraftment of human ES cell-derived dopaminergic neurons enriched by coculture with telomerase-immortalized midbrain astrocytes. Nat. Med. *12*, 1259–1268.

Roybon, L., Lamas, N.J., Garcia-Diaz, A., Yang, E.J., Sattler, R., Jackson-Lewis, V., Kim, Y.A., Kachel, C.A., Rothstein, J.D., Przedborski, S., et al. (2013). Human stem cell-derived spinal cord astrocytes with defined mature or reactive phenotypes. Cell Reports *4*, 1035–1048.

Serio, A., Bilican, B., Barmada, S.J., Ando, D.M., Zhao, C., Siller, R., Burr, K., Haghi, G., Story, D., Nishimura, A.L., et al. (2013). Astrocyte pathology and the absence of non-cell autonomy in an induced pluripotent stem cell model of TDP-43 proteinopathy. Proc. Natl. Acad. Sci. USA *110*, 4697–4702.

Shaltouki, A., Peng, J., Liu, Q., Rao, M.S., and Zeng, X. (2013). Efficient generation of astrocytes from human pluripotent stem cells in defined conditions. Stem Cells *31*, 941–952.

Sofroniew, M.V. (2014). Multiple roles for astrocytes as effectors of cytokines and inflammatory mediators. Neuroscientist *20*, 160–172.

Sofroniew, M.V., and Vinters, H.V. (2010). Astrocytes: biology and pathology. Acta Neuropathol. *119*, 7–35.

Son, E.Y., Ichida, J.K., Wainger, B.J., Toma, J.S., Rafuse, V.F., Woolf, C.J., and Eggan, K. (2011). Conversion of mouse and human fibroblasts into functional spinal motor neurons. Cell Stem Cell *9*, 205–218.

Takahashi, K., and Yamanaka, S. (2006). Induction of pluripotent stem cells from mouse embryonic and adult fibroblast cultures by defined factors. Cell *126*, 663–676.

Tanaka, N., Morita, T., Nezu, A., Tanimura, A., Mizoguchi, I., and Tojyo, Y. (2003). Thrombin-induced Ca2+ mobilization in human gingival fibroblasts is mediated by protease-activated receptor-1 (PAR-1). Life Sci. *73*, 301–310.

Theka, I., Caiazzo, M., Dvoretskova, E., Leo, D., Ungaro, F., Curreli, S., Managò, F., Dell'Anno, M.T., Pezzoli, G., Gainetdinov, R.R., et al. (2013). Rapid generation of functional dopaminergic neurons from human induced pluripotent stem cells through a single-step procedure using cell lineage transcription factors. Stem Cells Transl. Med. *2*, 473–479.

Ubl, J.J., and Reiser, G. (1997). Characteristics of thrombin-induced calcium signals in rat astrocytes. Glia *21*, 361–369.

Valente, P., Fernández-Carvajal, A., Camprubí-Robles, M., Gomis, A., Quirce, S., Viana, F., Fernández-Ballester, G., González-Ros, J.M., Belmonte, C., Planells-Cases, R., et al. (2011). Membrane-tethered peptides patterned after the TRP domain (TRPducins) selectively inhibit TRPV1 channel activity. FASEB J. *25*, 1628–1640.

Vierbuchen, T., Ostermeier, A., Pang, Z.P., Kokubu, Y., Südhof, T.C., and Wernig, M. (2010). Direct conversion of fibroblasts to functional neurons by defined factors. Nature *463*, 1035–1041.

Yang, N., Zuchero, J.B., Ahlenius, H., Marro, S., Ng, Y.H., Vierbuchen, T., Hawkins, J.S., Geissler, R., Barres, B.A., and Wernig, M. (2013). Generation of oligodendroglial cells by direct lineage conversion. Nat. Biotechnol. *31*, 434–439.

Yoo, A.S., Sun, A.X., Li, L., Shcheglovitov, A., Portmann, T., Li, Y., Lee-Messer, C., Dolmetsch, R.E., Tsien, R.W., and Crabtree, G.R. (2011). MicroRNA-mediated conversion of human fibroblasts to neurons. Nature *476*, 228–231.

Zhou, M., Schools, G.P., and Kimelberg, H.K. (2006). Development of GLAST(+) astrocytes and NG2(+) glia in rat hippocampus CA1: mature astrocytes are electrophysiologically passive. J. Neurophysiol. *95*, 134–143.